Clebsch-type coordinates for nonlinear gyrokinetics in generic toroidal configurations

P. Xanthopoulos
Max-Planck-Institut für Plasmaphysik, Teilinstitut Greifswald, Wendelsteinstr. 1, D-17491 Greifswald, Germany

F. Jenko
Max-Planck-Institut für Plasmaphysik, Boltzmannstr. 2, D-85748 Garching, Germany

(Received 12 June 2006; accepted 26 July 2006; published online 7 September 2006)

The nonlinear gyrokinetic equations are frequently used as a basis for simulations of small-scale turbulence in magnetized toroidal plasmas. In this context, field-aligned coordinates are usually employed in order to minimize the number of necessary grid points. The present work proposes a system of Clebsch-type coordinates which does not depend on the existence of flux surfaces. The construction and use of these coordinates is explained, and the corresponding formulation of the nonlinear gyrokinetic equations is accomplished. This setup paves the way toward the investigation of nonaxisymmetric toroidal geometries, also in the region of magnetic islands as well as inside the ergodic layer where flux surfaces cease to exist. For testing purposes, in the axisymmetric, large aspect ratio case, the well-known $\hat{s}$-α expressions are recovered for closed flux surfaces. Moreover, geometric data for a specific stellarator configuration are computed and discussed.
 [DOI: 10.1063/1.2338818]

I. INTRODUCTION

One of the key challenges in modern fusion research is to theoretically understand and predict the properties of small-scale turbulence in magnetized toroidal plasmas. Especially since the advent of large supercomputers, significant progress could be achieved in this area of research by means of massively parallel codes based on the nonlinear gyrokinetic equations.[1–4] Such computations are often performed in field-line following coordinates using toroidal flux tubes[5–7] in order to minimize the number of necessary grid points.

Given the fact that turbulent fluctuations tend to have parallel correlation lengths which exceed their perpendicular counterparts by many orders of magnitude,[8] it often suffices (at least in tokamak geometry) to use only about 20 grid points along the field line to cover an entire connection length distance of $2\pi qR$. (Here, q and R denote, respectively, the safety factor and the major radius.) This is in stark contrast to the perpendicular directions for which the grid spacing is usually chosen to be of the order of the thermal ion gyroradius ρ_i. If one would use a grid which does not exploit the elongated nature of the turbulence, the grid spacing in the third coordinate direction would also have to be close to ρ_i. Thus, by using field-aligned coordinates, one can reduce the computational effort by a factor of about $R/\rho_i \sim 10^2 - 10^3$.

In the present paper, we introduce, construct, and utilize a system of Clebsch-type coordinates, without presupposing the existence of magnetic surfaces. From a purely geometrical viewpoint, this feature is an important prerequisite for the investigation of general magnetic topologies, including islands and the ergodic region. Of course, one should additionally take into account the physical implications imposed by this generalization, in terms of the relevant gyrokinetic orderings. Another nontrivial point is the determination of background conditions, as expressed by the density and temperature gradients. A thorough discussion of these issues, based on realistic magnetic configurations, will appear in a forthcoming work.

The remainder of this paper is structured as follows. In Sec. II, we explain the construction and use of Clebsch-type coordinates in generic magnetic field topologies. In particular, we will show how to compute the metric elements and the Jacobian, starting from a simple cylindrical coordinate system. In Sec. III, we then derive the form of various differential operators occurring in nonlinear gyrokinetics. In this context, we use a normalized version of the gyrokinetic equations which also forms the basis for the gyrokinetic turbulence code GENE (Refs. 9 and 10). Next, in Sec. IV, it will be shown that in the axisymmetric, large aspect ratio case, the well-known $\hat{s}$-α expressions are recovered. Moreover, geometric data for the W7-X stellarator configuration are computed and discussed. Finally, we draw some conclusions and provide an outlook in Sec. V.

II. CLEBSCH-TYPE COORDINATES

As is widely known, turbulence computations benefit greatly from the use of field-aligned coordinate systems. (We just note in passing that the same is also true for Braginskii-like systems dealing with large anisotropies, see, e.g., Ref. 11.) Since the turbulent fluctuations tend to have parallel correlation lengths which exceed their perpendicular counterparts by many orders of magnitude, the number of necessary grid points can thus be minimized. In the present section, we will introduce a system of Clebsch-type coordinates. These are generated through a transformation from the usual cylindrical system (r,z,ϕ) (here, ϕ denotes the toroidal angle) to the system

$$(v^1, v^2, \tau) \tag{1}$$

via field-line tracing. In this context, v^1 and v^2 are Clebsch-type coordinates with dimension of length and τ is an angle-like coordinate following the field line.

By construction, for the contravariant components of the magnetic field, we have

$$B^1 = B^2 = 0 \tag{2}$$

and, as will be explained shortly,

$$B^\tau = B^\phi. \tag{3}$$

Subsequently, the magnetic field can be expressed as

$$\mathbf{B} = JB^\phi \nabla v^1 \times \nabla v^2, \tag{4}$$

where J is the Jacobian of the system, defined by $J^{-1} = \nabla v^1 \times \nabla v^2 \cdot \nabla \tau$. Obviously, Eq. (4) is consistent with Eqs. (2) and (3). This coordinate system bears the following special properties:

(1) It does *not* presuppose the existence of magnetic surfaces, thus allowing for the investigation of ergodic regions, present in both tokamak (e.g., Tore Supra,[12] Tokamak EXperiment for Technology Oriented Research[13]) and stellarator [e.g., Wendelstein 7-X (Ref. 14)] configurations.
(2) The quantity JB^ϕ is a *stream function* (i.e., a constant along the field line), but, in principle, its value may vary from one field line to another (in contrast, for standard flux coordinates, this quantity characterizes a magnetic surface).

After this brief introduction, we will now discuss the construction of (v^1, v^2, τ) coordinates in more detail.

A. Construction of the coordinate system

We aim at setting up coordinates (v^1, v^2, τ), which are aligned to an arbitrary magnetic field configuration. To achieve this, we follow a constructive method which identifies v^1 and v^2 as Clebsch-type coordinates. In other words, these two coordinates determine a certain field line, while the third coordinate τ locates the position along the field line. In this way, three-dimensional space is appropriately parametrized.

Clebsch-type coordinates v^1 and v^2 can be defined by means of a well-known constructive method which is explained, e.g., in Ref. 15. For concreteness, we consider the poloidal surface $\phi = \phi_0$ on which the r=const and z=const curves generate a Cartesian grid. Now, each point (r,z) in a certain region of interest can be viewed as the starting point of a magnetic field line, and thus the isolines of r and z in the $\phi = \phi_0$ plane turn into two-dimensional "magnetic surfaces" (not necessarily in the sense of flux surfaces). The surfaces containing the point $(r,z) = (r_i, z_j)$ shall be described by the equations $v^1(\mathbf{R}) = 0$ and $v^2(\mathbf{R}) = 0$, respectively, where $\mathbf{R}$ denotes the spatial position vector. The magnetic field line passing through the grid point (r_i, z_j, ϕ_0) can then be envisaged as the intersection of these two surfaces. At this point, it should be noted, however, that the above choice of Clebsch-type coordinates $v^1$and v^2 is not unique. One can also define other families of "magnetic surfaces" which might be more suitable. For example, in the presence of flux surfaces, it is usually advantageous to choose one of the two Clebsch coordinates to be a flux-surface label. This particular aspect is discussed in more detail later in the text as well as in the Appendix.

In order to complete the parametrization of the field line, we introduce a third coordinate with the property that the corresponding covariant vector is tangent to the field line. In the standard Clebsch setup, this coordinate is the arc length ℓ. In our case, however, we select another coordinate, namely τ, which is related to the arc length through the expression

$$\ell'(\tau) = \frac{B}{B^\phi}, \tag{5}$$

meaning that τ is not a physical parameter for the representation of the field line. The reason for this specific choice is attributed to the fact that τ is an angle-like coordinate, which has a very close connection to the toroidal angle ϕ. Indeed, from the equation for the field line with respect to the cylindrical coordinates, one gets

$$\frac{d\phi}{d\ell} = \frac{B^\phi}{B}, \tag{6}$$

which, combined with (5), yields $d\tau = d\phi$. Using $\tau(0) = \phi_0$ as initial condition and integrating, we end up with the simple expression $\tau = \phi - \phi_0$.

In conclusion, the coordinate system (v^1, v^2, τ) constructed this way satisfies Eq. (2), i.e., the vector $\mathbf{e}_\tau$ is parallel to $\mathbf{B}$, as well as Eq. (3), since it holds

$$B^\tau = \mathbf{B} \cdot \nabla_\tau = \mathbf{B} \cdot \nabla \phi = B^\phi. \tag{7}$$

B. Calculation of the metric elements

The coordinate system (v^1, v^2, τ) is characterized, in large part, by its metric elements. In the following, we present a method for computing these quantities, which can be considered as a generalization of Ref. 16, in the sense that we no longer presuppose the existence of magnetic surfaces.

For convenience, we introduce the notation $(y^1, y^2, y^3) = (r, z, \phi)$ and $v^3 = \tau$. The goal, then, is to determine the derivatives

$$C_j^l \equiv \frac{\partial v^l}{\partial y^j} \quad (j,l = 1,2,3), \tag{8}$$

so that we can proceed with the transformation

$$g^{kl} = \sum_{i,j=1}^{3} g_c^{ij} C_i^k C_j^l, \quad \text{where } g_c = \text{diag}\{1, 1, r^{-2}\}. \tag{9}$$

The first step toward this goal consists of rewriting Eq. (2) as

$$\mathbf{B} \cdot \nabla v^l = 0 \quad (l = 1,2) \tag{10}$$

or

$$\sum_{k=1}^{3} B_c^k C_k^l = 0 \quad (l=1,2), \tag{11}$$

where $B_c^k (k=1,2,3)$ are the contravariant cylindrical components. Now, we differentiate Eq. (11) with respect to $y^j (j=1,2,3)$ and obtain

$$\sum_{k=1}^{3} B_c^k \frac{\partial C_j^l}{\partial y^k} = -\sum_{k=1}^{3} C_k^l \frac{\partial B_c^k}{\partial y^j} \quad (l=1,2). \tag{12}$$

Here, we have tacitly used the relation

$$\frac{\partial C_k^l}{\partial y^j} = \frac{\partial C_j^l}{\partial y^k}, \tag{13}$$

which acts as a smoothing constraint, namely $v^l \in C^2$ $(l=1,2)$.

At this stage, we will transform the system of partial differential equations (12) to a corresponding system of ordinary differential equations by employing the field-line equation in cylindrical coordinates. In terms of the coordinate τ, this equation reads

$$\frac{dy^k}{d\tau} = \ell'(\tau)\frac{B_c^k}{B} \quad (k=1,2,3). \tag{14}$$

Thus, combining Eqs. (12) and (14), we obtain

$$\frac{d}{d\tau} C_j^l = -\ell'(\tau) \sum_{k=1}^{3} \frac{C_k^l}{B} \frac{\partial B_c^k}{\partial y^j} \quad (l=1,2; j=1,2,3) \tag{15}$$

and, in view of Eq. (5), Eq. (15) takes the final form

$$\frac{d}{d\tau} C_j^l = -\sum_{k=1}^{3} \frac{C_k^l}{B^\phi} \frac{\partial B_c^k}{\partial y^j} \quad (l=1,2; j=1,2,3). \tag{16}$$

In addition, we have

$$C_1^3 = C_2^3 = 0 \quad \text{and} \quad C_3^3 = 1. \tag{17}$$

The initial conditions for this system of equations on the surface $\phi=\phi_0$ are deduced from the assumption that the Clebsch coordinate lines $v^1=$const and $v^2=$const at the starting point are tangential to the isolines of the cylindrical coordinates r and z, so that

$$C_n^m(\tau=0) = \delta_n^m \quad (m,n=1,2). \tag{18}$$

The remaining initial conditions can be prescribed only implicitly by means of Eq. (11),

$$C_3^1(\tau=0) = -\frac{B^r}{B^\phi}, \quad C_3^2(\tau=0) = -\frac{B^z}{B^\phi}. \tag{19}$$

The quantities $C_j^i (i,j=1,2,3)$ can thus be computed by solving the system of Eqs. (16)–(19) numerically, employing, e.g., a higher-order Runge-Kutta scheme. Using Eq. (9), one then obtains the metric elements g^{kl} associated with the constructed coordinate system.

As a final remark, we note that, in the case of nested flux surfaces, it is always possible to build up a flux coordinate system from the presented algorithm, in the sense that one of the coordinates is a flux-surface label. However, this is *not* guaranteed by the initial conditions (19). In fact, it turns out that, even for the simple geometry of circular flux surfaces, these conditions fail to construct a flux coordinate system. Nevertheless, there is one exception to this general rule; namely, if the tracing procedure starts in the symmetry plane (see Appendix for analytical proof). There, it holds $B^r=0$ and the initial conditions (19) take the special form

$$C_3^1(\tau=0) = 0, \quad C_3^2(\tau=0) = -\frac{B^z}{B^\phi}, \tag{20}$$

so that the coordinate v^1 becomes a flux-surface label. In fact, it is through this procedure that we generate a flux coordinate system for the circular tokamak case presented later.

C. Calculation of the Jacobian

Another important piece of geometrical information is contained in the Jacobian of the coordinate system. The latter is numerically determined via application of the chain rule

$$J = J_c \left| \frac{\partial(y^1,y^2,y^3)}{\partial(v^1,v^2,\tau)} \right| = r \left| \frac{\partial(y^1,y^2,y^3)}{\partial(v^1,v^2,\tau)} \right|, \tag{21}$$

where J_c denotes the Jacobian for the cylindrical system. To compute the determinant, we need to solve a system of ordinary differential equations similar to Eqs. (16)–(19). Specifically, setting

$$D_j^i \equiv \frac{\partial y^i}{\partial v^j} \quad (i,j=1,2,3), \tag{22}$$

we notice that

$$\sum_{k=1}^{3} D_k^l C_m^k = \delta_m^l. \tag{23}$$

Now, differentiating with respect to τ and using Eq. (16), we readily obtain

$$\frac{d}{d\tau} D_j^l = \sum_{k=1}^{3} \frac{D_j^k}{B^\phi} \frac{\partial B_c^l}{\partial y^k} \quad (l,j=1,2). \tag{24}$$

In addition, we have

$$D_1^3 = D_2^3 = 0, \quad D_3^3 = 1, \quad D_3^1 = \frac{B^r}{B^\phi}, \quad D_3^2 = \frac{B^z}{B^\phi}. \tag{25}$$

In the same spirit as before, we employ as initial conditions on the $\phi=\phi_0$ surface

$$D_n^m(\tau=0) = \delta_n^m \quad (m,n=1,2). \tag{26}$$

D. The stream function

We would like to close the present section by demonstrating that, in the context of our coordinates, the quantity JB^ϕ is constant on each field line, while its value may change from one field line to another. We begin with rewriting Eq. (10) in the equivalent form

$$\mathbf{B} = K \nabla v^1 \times \nabla v^2, \tag{27}$$

where $K=K(v^1,v^2,\tau)$. By imposing that the magnetic field be divergence free, the dependence of K on τ can be removed. Indeed,

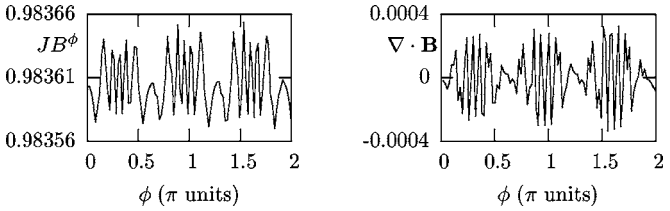

FIG. 1. The stream function JB^{ϕ} along a magnetic field line. The numerical noise merely reflects the small deviation from $\nabla \cdot \mathbf{B}=0$ in the equilibrium data.

$$0 = \nabla \cdot \mathbf{B} = \nabla v^1 \times \nabla v^2 \cdot \nabla K = K^{-1}\mathbf{B} \cdot \nabla K, \tag{28}$$

which implies that

$$\frac{d}{d\tau}K = 0. \tag{29}$$

Furthermore, recalling that $B^{\tau}=B^{\phi}$ and $J^{-1}=\nabla v^1 \times \nabla v^2 \cdot \nabla \tau$, we obtain the expression $K=JB^{\phi}$. Thus, we have

$$\frac{d}{d\tau}JB^{\phi} = 0. \tag{30}$$

Integrating this relation, it follows immediately that the quantity JB^{ϕ} is actually a stream function, with its value dictated by the initial condition on the surface $\phi=\phi_0$. A numerical example is shown in Fig. 1.

III. APPLICATION TO NONLINEAR GYROKINETICS

In this section, we will derive the form of various differential operators occurring in nonlinear gyrokinetics. In this context, we use a normalized version of the gyrokinetic equations which is used in the gyrokinetic turbulence code GENE (Refs. 9 and 10). We thus specify in which way the geometrical information enters the problem, when using the above constructed coordinates for an arbitrary toroidal magnetic field.

A. The gyrokinetic Vlasov equation

The independent and dependent variables are normalized, respectively, according to Tables I and II (as velocity space coordinates, we employ the parallel velocity $v_{\parallel}$ and the magnetic moment μ). Here, we have used the ion sound scale $\rho_s=c_s/\Omega_i$, the ion Larmor frequency $\Omega_i=eB_{\mathrm{ref}}/m_i c$, the ion sound speed $c_s=\sqrt{T_{e0}/m_i}$, the thermal velocity $v_{T_j}=\sqrt{2T_{j0}/m_j}$ of species $j(j=\mathrm{e},\mathrm{i})$, the safety factor q, a typical perpendicular equilibrium scale length $L_{\perp}$, and a characteristic length R_{ref}. The latter is set usually equal to the major radius, but, in principle, it can be chosen arbitrarily, as long as it is used consistently everywhere. The normalization for the potentials Φ and $A_{\parallel}$ is a direct consequence of the typical gyrokinetic ordering (see, also, Refs. 17 and 18)

TABLE I. Normalization of the independent variables.

t	$\nabla_{\perp}$	$\nabla_{\parallel}$	$v_{\parallel}$	μ
$L_{\perp}/c_s$	ρ_s	qR_{ref}	v_{T_j}	T_{j0}/B_{ref}

TABLE II. Normalization of the dependent variables.

F_{j0}	F_{j1}	Φ	$A_{\parallel}$
$n_0/v_{T_j}^3$	$(n_0/v_{T_j}^3)\rho_s/L_{\perp}$	$(T_{e0}/e)\rho_s/L_{\perp}$	$(qR_{\mathrm{ref}}\rho_s B_{\mathrm{ref}}\beta_e/L_{\perp})\rho_s/L_{\perp}$

$$\frac{e\Phi}{T_{e0}} \sim \frac{A_{\parallel}}{\rho_s B_{ref}} = \mathcal{O}\left(\frac{\rho_s}{L_{\perp}}\right).$$

Notice that the equilibrium magnetic field is normalized with respect to B_{ref}, to be specified later.

In vector form, the (normalized) gyrokinetic Vlasov equation for the perturbed part F_{j1} of the distribution function F_j then reads

$$\begin{aligned}\frac{\partial g_j}{\partial t} &- \left(\boldsymbol{\omega}_n + \boldsymbol{\omega}_{T_j}\left(v_{\parallel}^2 + \mu B - \frac{3}{2}\right)\right)F_{j0}\cdot \mathbf{b}\times\frac{\nabla\chi_j}{B} \\ &+ \mathbf{b}\times\frac{\nabla\chi_j}{B}\cdot\nabla G_j + \frac{1}{\sigma_j}(\mu B + 2v_{\parallel}^2)\mathbf{b}\times\frac{\nabla B}{B^2}\cdot\nabla G_j \\ &+ \alpha_j v_{\parallel}\nabla_{\parallel}G_j - \frac{\alpha_j}{2}\mu\nabla_{\parallel}B\frac{\partial F_j}{\partial v_{\parallel}} = 0,\end{aligned} \tag{31}$$

where we have used the definitions (gyroaveraged quantities are denoted by overbars)

$$g_j = F_{j1} + \sigma_j\alpha_j v_{\parallel}F_{j0}\hat{\epsilon}\beta_e\bar{A}_{1\parallel}, \quad G_j = g_j + \sigma_j\chi_j F_{j0},$$

$$\chi_j = \bar{\Phi}_1 - \alpha_j v_{\parallel}\hat{\epsilon}\beta_e\bar{A}_{1\parallel},$$

as well as

$$\sigma_j = \frac{e_j}{e}\frac{T_{e0}}{T_{j0}}, \quad \alpha_j = \frac{v_{T_j}}{c_s}\frac{L_{\perp}}{qR_{\mathrm{ref}}}, \quad \hat{\epsilon} = \left(\frac{qR_{\mathrm{ref}}}{L_{\perp}}\right)^2,$$

$$\beta_e = \frac{4\pi n_0 T_{e0}}{B_{\mathrm{ref}}^2},$$

$$\boldsymbol{\omega}_n = (\mathbf{bb}-\mathbf{I})\cdot\frac{\nabla n}{n}, \quad \boldsymbol{\omega}_{T_j} = (\mathbf{bb}-\mathbf{I})\cdot\frac{\nabla T_j}{T_j}.$$

The gyroaveraging procedure for species j is performed, as usual, via the Bessel function $J_0(\lambda_j)$, where the (square of the) argument λ_j, with respect to the Clebsch system, is defined later. As equilibrium distribution we take a Maxwellian which reads

$$F_{j0}(v_{\parallel},\mu) = \pi^{-3/2}e^{-(v_{\parallel}^2+\mu B)}$$

in normalized units.

In most existing works, Eq. (31) is expressed in Boozer-type coordinate systems, based on flux surfaces, with the additional assumption of axisymmetry. The simple $\hat{s}$-α model[19] for axisymmetric toroidal equilibria is covered, e.g., in Ref. 10. Here, we attempt to provide a generic form instead, which is also suitable for *nonaxisymmetric* toroidal devices and situations *without nested flux surfaces*. To this aim, we express the (normalized) differential operators occurring in Eq. (31) in the (v^1, v^2, τ) coordinate system. For any quantities A and G, we have

$$\mathbf{b}\times\nabla A\cdot\nabla G = Jb^3[(g^{11}g^{22}-(g^{12})^2)\{\partial_1 A,\partial_2 G\} + (g^{11}g^{23}-g^{12}g^{13})\{\partial_1 A,\partial_3 G\} + (g^{12}g^{23}-g^{22}g^{13})\{\partial_2 A,\partial_3 G\}] \quad (32)$$

in terms of the commutator bracket

$$\{\partial_i A,\partial_j G\} = \partial_i A\partial_j G - \partial_j A\partial_i G \quad (i,j=1,2,3) \quad (33)$$

and $b^3=\mathbf{b}\cdot\nabla\tau=B^\phi/B$. Here, J and b^3 have the dimensions of length and inverse length, respectively, while the metric elements g^{11}, g^{12}, and g^{22} are dimensionless quantities. In view of the usual ordering $k_\parallel \ll k_\perp$, Eq. (32) can be simplified by ignoring all terms that contain parallel gradients of fluctuating quantities. The same applies to the terms involving the parallel gradient of the magnetic field. However, for complex geometries, it is good practice to justify numerically this approximation. Furthermore, τ is replaced by qz, where q is the safety factor and z turns into the poloidal angle θ for simple geometries. Hence, z now plays the role of the parallel coordinate and the (normalized) parallel derivative takes the form

$$\nabla_\parallel = qR_{\mathrm{ref}}b^3\frac{\partial}{\partial\tau} = R_{\mathrm{ref}}b^3\frac{\partial}{\partial z}. \quad (34)$$

Consequently, in (v^1,v^2,z) coordinates, the gyrokinetic Vlasov equation reads

$$\begin{aligned}&\frac{\partial g_j}{\partial t}+\frac{\mathcal{M}\hat{b}^3}{B}\left(\frac{\partial\chi_j}{\partial v^1}\frac{\partial G_j}{\partial v^2}-\frac{\partial\chi_j}{\partial v^2}\frac{\partial G_j}{\partial v^1}\right)\\ &\quad+\frac{\mathcal{M}\hat{b}^3}{B}F_{j_0}\left(\omega_{n,1}+\omega_{T_j,1}\left(v_\parallel^2+\mu B-\frac{3}{2}\right)\right)\frac{\partial\chi_j}{\partial v^2}\\ &\quad-\frac{\mathcal{M}\hat{b}^3}{B}F_{j_0}\left(\omega_{n,2}+\omega_{T_j,2}\left(v_\parallel^2+\mu B-\frac{3}{2}\right)\right)\frac{\partial\chi_j}{\partial v^1}\\ &\quad+\frac{1}{2\sigma_j}(\mu B+2v_\parallel^2)\left(\mathcal{K}_1\frac{\partial G_j}{\partial v^1}+\mathcal{K}_2\frac{\partial G_j}{\partial v^2}\right)\\ &\quad+\alpha_j v_\parallel\hat{b}^3\frac{\partial G_j}{\partial z}-\frac{\alpha_j}{2}\mu\hat{b}^3\frac{\partial B}{\partial z}\frac{\partial F_j}{\partial v_\parallel}=0,\end{aligned} \quad (35)$$

where

$$\mathcal{M}=\hat{J}(g^{11}g^{22}-(g^{12})^2),\quad \hat{J}=J/R_{\mathrm{ref}},\quad \hat{b}^3=R_{\mathrm{ref}}b^3 \quad (36)$$

and

$$\omega_{n,k}=-\frac{L_\perp}{n}\frac{\partial n}{\partial v^k},\quad \omega_{T_j,k}=-\frac{L_\perp}{T_j}\frac{\partial T_j}{\partial v^k},\quad (k=1,2). \quad (37)$$

In addition, the curvature operators read

$$\mathcal{K}_1=-c_v\frac{\mathcal{M}\hat{b}^3}{B}\frac{R_{\mathrm{ref}}}{B}\frac{\partial B}{\partial v^2},\quad \mathcal{K}_2=c_v\frac{\mathcal{M}\hat{b}^3}{B}\frac{R_{\mathrm{ref}}}{B}\frac{\partial B}{\partial v^1},\quad c_v=\frac{2L_\perp}{R_{\mathrm{ref}}}. \quad (38)$$

Note that in Eqs. (37) and (38), v^1 and v^2 are *not* normalized, and therefore the prefactors $L_\perp$ and R_{ref} enter the equations. This is in contrast to Eq. (35), where v^1 and v^2 are dimensionless.

In the above equations, the expression $\mathcal{M}\hat{b}^3/B$ occurs several times and shall be examined a little further here. Using the representation (4) (also true for the normalized equilibrium magnetic field), we obtain

$$B^2=(JB^\phi)^2(g^{11}g^{22}-(g^{12})^2), \quad (39)$$

which is equivalent to

$$\frac{\mathcal{M}\hat{b}^3}{B}=\frac{B_{\mathrm{ref}}}{JB^\phi}=\mathrm{const} \quad (40)$$

due to Eq. (30). Thus we can eliminate the term $\mathcal{M}\hat{b}^3/B$ from Eqs. (35) and (38) by postulating

$$B_{\mathrm{ref}}=JB^\phi. \quad (41)$$

In this case, we then have

$$\hat{b}^3=\frac{1}{\hat{J}B}. \quad (42)$$

Having completed the derivation of the Vlasov equation, the following remarks are in place:

- The form of Eq. (35) is invariant with respect to the interchange of the coordinates v^1 and v^2. This results from the fact that the coordinate system (v^2,v^1,z) is left-handed, and therefore the corresponding Jacobian (hidden in $\mathcal{M}$) becomes negative.
- The form of Eq. (35) is invariant with respect to the choice of Clebsch-type coordinates. Indeed, for a specific magnetic line, two different systems differ only in the value of the stream function JB^ϕ, which is absorbed by the normalization procedure by setting it equal to B_{ref}. However, for each coordinate system, the expressions for the gradients $\omega_{n,k},\omega_{T_j,k}$ will have to be modified accordingly. Thus, for a coordinate system in the presence of nested surfaces, with v^1 (or v^2) as a flux-surface label, the fourth (or third) term is suppressed. In a different situation, e.g., in an ergodic region, both contributions should be retained.

In summary, the magnetic geometry enters the gyrokinetic Vlasov equation essentially in three ways—through the magnetic field strength B, through the Jacobian J, and through the magnetic curvature terms $\mathcal{K}_1$ and $\mathcal{K}_2$. In the framework of a flux tube approach, all of these quantities are solely functions of the parallel coordinate z.

B. The gyrokinetic field equations

The self-consistent electromagnetic field is determined via the gyrokinetic Poisson equation

$$\sum_j e_j\sigma_j(1-\Gamma_0(b_j))\Phi=\sum_j \pi e_j B\int d\mu dv_\parallel J_0(\lambda_j)g_j \quad (43)$$

and the gyrokinetic Ampère's law

$$\left(\nabla_\perp^2 - \frac{1}{2}\hat{\epsilon}\beta_e \sum_j \sigma_j \alpha_j^2 \frac{e_j}{e}\Gamma_0(b_j)\right)A_\parallel$$

$$= -\sum_j \pi\alpha_j \frac{e_j}{e} B \int d\mu dv_\parallel J_0(\lambda_j) v_\parallel g_j. \tag{44}$$

Here, the Bessel function J_0 and the function $\Gamma_0(b_j) = e^{-b_j} I_0(b_j)$ (where I_0 is the modified Bessel function) have been introduced. The arguments λ_j and b_j are defined, respectively, as

$$b_j = -\frac{T_j}{T_e}\frac{m_j}{m_i}\frac{e^2}{e_j^2}\frac{1}{B^2}\nabla_\perp^2, \quad \lambda_j^2 = 2\mu B b_j. \tag{45}$$

The magnetic geometry enters these equations through the perpendicular Laplacian which is defined as

$$\nabla_\perp^2 A = \frac{1}{J}\sum_{i,j=1}^{2} \partial_i (J g^{ij} \partial_j A). \tag{46}$$

For a flux tube simulation, the Jacobian and the metric elements are functions of the parallel coordinate only, and therefore this expression reduces to

$$\nabla_\perp^2 A = \sum_{i,j=1}^{2} g^{ij} \partial_i \partial_j A. \tag{47}$$

In summary, the magnetic geometry enters the gyrokinetic field equations through the magnetic field strength B and through the elements g^{11}, g^{12}, and g^{22} of the metric tensor.

IV. TWO TEST CASES

In this section, we examine two test cases. First, it is demonstrated that our coordinate approach reproduces the well-known $\hat{s}$-α model results for a tokamak with large aspect ratio. Next, we generate the geometrical data for the stellarator device W7-X and compare it to the tokamak case.

A. Large aspect ratio, circular tokamak

In order to test our concept of coordinates as previously described, we first want to apply it to a regime in which the numerical results can be directly compared with analytical ones. Therefore, we study the case of a large aspect ratio tokamak with circular cross section and no Shafranov shift (α=0). Here, the metric elements and the curvature terms are given by the expressions[7,19]

$$g^{11}(z) = 1, \quad g^{12}(z) = \hat{s}z, \quad g^{22}(z) = 1 + (\hat{s}z)^2 \tag{48}$$

and

$$\mathcal{K}_1(z) = -\sin z, \quad \mathcal{K}_2(z) = -(\cos z + \hat{s}z \sin z), \tag{49}$$

where $\hat{s} \equiv (r/q)(dq/dr)$ characterizes the magnetic shear, and the curvature parameter $c_v = 2L_\perp / R_{\mathrm{ref}}$ is set to unity (thus defining $L_\perp$).

These analytical results are now to be compared to numerical results obtained from a magnetohydrodynamic equilibrium via our coordinate approach. As an example, we examine the metric elements and the curvature terms for a tokamak with a major radius of R=3.0 m and a minor radius of a=0.25 m for a magnetic surface with ρ/a=0.2, q=2.55, and $\hat{s}$=0.187. The traced field line starts in the outboard midplane, i.e., at r_0=3.05 m (and $z_0 = \phi_0$=0), and we choose $R_{\mathrm{ref}} = r_0$. As can be seen in Figs. 2 and 3, the agreement with Eqs. (48) and (49) is excellent. (Actually, the respective curves are practically identical.) Here, the cylindrical coordinate r describes the distance from the symmetry axis and, in the present case, is given by $r(z) = R + \rho\cos z$.

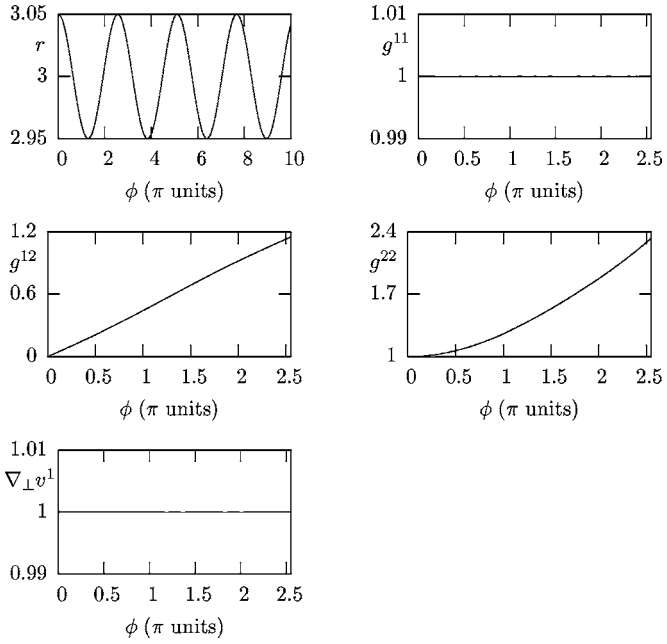

FIG. 2. Distance r (in m) from the symmetry axis and metric elements g^{11}, g^{12}, and g^{22} as computed numerically from a magnetohydrodynamic equilibrium via our coordinate approach. It is also demonstrated that the Clebsch-type system corresponds, in this case, to a flux coordinate system.

Since the analytical expressions (48) and (49) are based on a Boozer-type system, the presented results speak for the validity of the aforementioned remark in Sec. II B about the construction of a flux coordinate system. In fact, this conclusion can also be inferred by the fact $\nabla_\perp v^1 = \mathbf{n}\cdot\nabla v^1 = 1$ (see Fig. 2), where $\mathbf{n}$ is the unit vector normal to the surface. In combination with $\|\nabla v^1\| = \sqrt{g^{11}} = 1$, it is evident that v^1 is indeed a flux-surface label.

Using the approximation

$$B_{\mathrm{tor}} \approx B \propto r^{-1}, \tag{50}$$

which is well satisfied for most tokamaks, two interesting conclusions can be drawn. First, the Jacobian obeys the relation

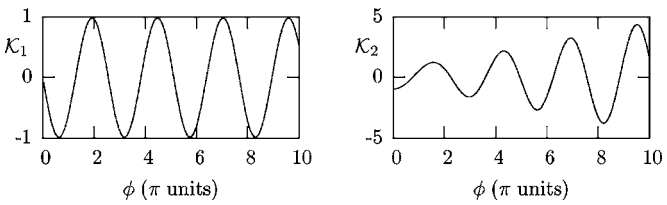

FIG. 3. Curvature terms $\mathcal{K}_1$ and $\mathcal{K}_2$ as computed numerically from a magnetohydrodynamic equilibrium via our coordinate approach.

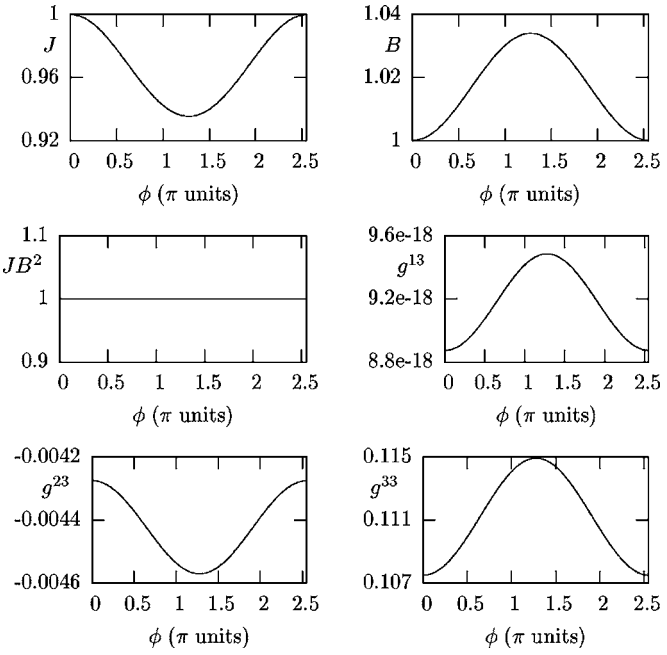

FIG. 4. Normalized Jacobian and magnetic field, as well as metric elements for a tokamak with $B_{\mathrm{tor}} \approx B$. One finds that $J \propto B^{-2}$ and $g^{33}=r^{-2} \gg g^{13}, g^{23}$. In particular, $B(z)=r_0/r(z)$ and $J(z)=[r(z)/r_0]^2$, as expected.

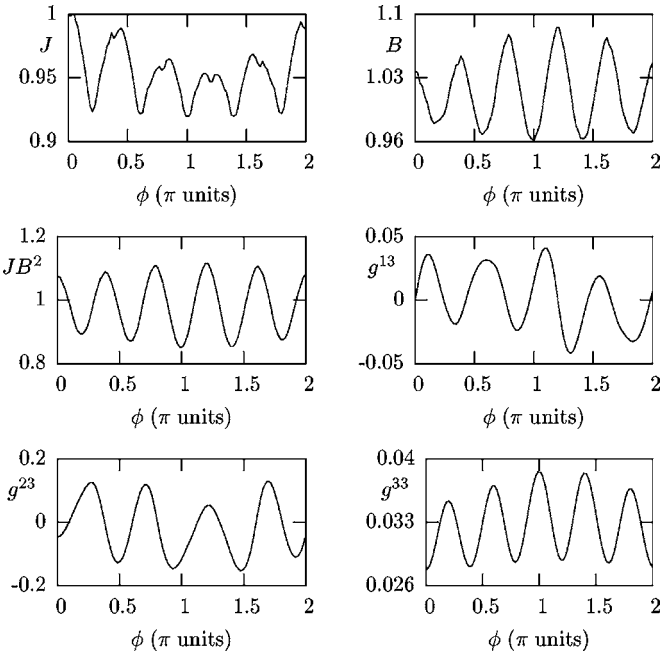

FIG. 5. Normalized Jacobian, magnetic field, as well as metric elements for the stellarator W7-X. The fivefold symmetry is clearly depicted. The Jacobian is no longer inversely proportional to B^2. Moreover, the relationship $g^{33} \gg g^{13}, g^{23}$ does not hold anymore.

$$J \propto B^{-2}, \tag{51}$$

since we have $J \propto 1/B^{\phi} \propto r/B_{\mathrm{tor}} \approx r/B \propto B^{-2}$. Second, one finds that

$$g^{33} = r^{-2} \gg g^{13}, g^{23}, \tag{52}$$

which stems from the relation (39). From this, successively, we get

$$\begin{aligned} \det[g^{rs}] = J^{-2} &= (B^{\phi}/B)^2 (g^{11}g^{22} - (g^{12})^2) \\ &= \left(\frac{B_{\mathrm{tor}}}{rB}\right)^2 (g^{11}g^{12} - (g^{12})^2) \\ &\approx r^{-2}(g^{11}g^{22} - (g^{12})^2) \\ &= g^{33}(g^{11}g^{22} - (g^{12})^2), \end{aligned} \tag{53}$$

which proves our claim. The validity of Eqs. (51) and (52), which holds for *any* tokamak (independent of its aspect ratio and cross section) satisfying Eq. (50), is confirmed in Fig. 4.

In conclusion, for a large aspect ratio, circular tokamak, the $\hat{s}$-α results are recovered by the coordinate approach described in the last two sections. Next, we will focus on a rather different magnetic geometry, namely that of the stellarator W7-X.

B. The stellarator W7-X

Next, we would like to study a vacuum field of the stellarator experiment W7-X, which has a major radius of $R=5.5$ m and a mirror of $a=0.53$ m. Despite the complicated three-dimensional structure of this configuration, the presented method of constructing the Clebsch-type coordinate system works equally well here. In order to demonstrate this, we compute the resulting geometrical information and compare it to that of the simple tokamak case presented in Sec. IV A. For the results shown below, we trace a field line starting in the outboard midplane $(r_0, z_0)=(6.0, 0)$ on the poloidal surface $\phi_0=0$ for a distance of one toroidal turn.

We start this comparison by noting that the approximation (50) fails for W7-X. Here, the poloidal field components are of the same order as the toroidal ones. Therefore, one should expect that Eqs. (51) and (52), describing the behavior of the Jacobian and the metric elements, no longer hold. The results displayed in Fig. 5 support this claim. To begin with, the metric elements g^{13} and g^{23} are not small anymore with respect to g^{33}, a characteristic which reveals the three dimensionality of the magnetic field. Furthermore, the quantity JB^2 is no longer constant, but rather a fluctuating function of the parallel coordinate which reflects the fivefold symmetry of the device.

As shown in Figs. 6 and 7, the parallel structure of the metric elements g^{11}, g^{12}, and g^{22}, as well as that of the curvature terms $\mathcal{K}_1$ and $\mathcal{K}_2$, deviates substantially from the respective tokamak results that have been presented in Figs. 2 and 3. The strongest differences between W7-X and the simple tokamak are observed for these three metric elements which enter the gyrokinetic field equations. They actually exhibit relatively small-scale fluctuations of order unity. This feature imposes the requirement for much better numerical resolution in the parallel direction in gyrokinetic simulations, thus increasing considerably the computational effort. Instead of using some 20 parallel grid points, as is often done for typical tokamak equilibria, we find that about 100 parallel grid points are usually necessary in W7-X geometry. Results from linear and nonlinear gyrokinetic simulations based on the Clebsch-type coordinate approach put forward in this paper will be presented in future publications.

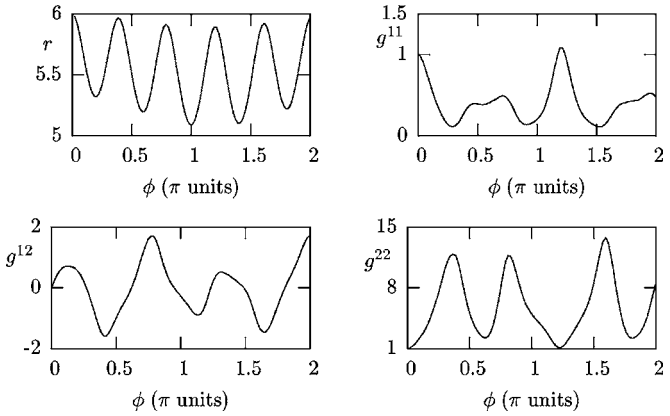

FIG. 6. Distance r (in m) from the symmetry axis and metric elements g^{11}, g^{12}, and g^{22} as computed numerically from a magnetohydrodynamic equilibrium via our coordinate approach. Notice that the values of the metric elements at $\phi=0$ correspond to the cylindrical ones, as dictated by the algorithm.

V. CONCLUSIONS AND OUTLOOK

In the context of computational studies of small-scale turbulence in magnetized toroidal plasmas, the nonlinear gyrokinetic equations are frequently used as a starting point. Here, it turns out to be of great importance to employ field-aligned coordinates in order to minimize the number of necessary grid points. Usually, one assumes that the magnetic configuration consists of a set of nested flux surfaces, and one chooses Clebsch-type coordinates, one of which is a flux-surface label. However, deviations from this standard scenario can occur. For example, it has long been known that stellarators tend to exhibit fairly large ergodic regions which can affect the plasma turbulence in a significant fashion. Moreover, there is a large number of tokamak experiments in which ergodicity also plays an important role. Under such conditions, the usual procedure breaks down and one has to come up with a new way of defining useful—and ideally still field-aligned—coordinate systems. This was the goal of the present work.

In this paper, we introduced a method for setting up Clebsch-type coordinates which has the advantage that it is not dependent on the existence of flux surfaces. Thus, in principle, it also applies to magnetic fields which may be characterized as ergodic or chaotic, at least in a static regime. The construction and use of these coordinates was explained in detail, and expressions for certain differential operators occurring in the nonlinear gyrokinetic equations were derived explicitly. For testing purposes, we then computed the respective geometrical data for a large aspect ratio tokamak with circular flux surfaces and no Shafranov shift. We found that the numerical results agree very well with the known analytical expressions. This fact demonstrates that the approach proposed in the present paper is merely a generalization of the usual ways of constructing field-aligned coordinates. In the presence of flux surfaces, the two approaches coincide, provided that the initial conditions for the field-line tracing are chosen appropriately.

Besides that, geometric data for the stellarator configuration W7-X were computed and discussed. Here, the most significant deviations from the tokamak case were found for the three metric elements which enter the gyrokinetic field equations. They actually exhibit relatively small-scale fluctuations in the field-line following coordinate of order unity. This very feature necessitates much better numerical resolution in the parallel direction (compared to a typical tokamak case) if one wants to perform gyrokinetic studies of microinstabilities and microturbulence in a configuration like W7-X. More concretely, the computational effort is higher by roughly an order of magnitude of more. [Here, one has to take into account that smaller parallel grid spacings also tend to demand smaller time steps (in light of the parallel Courant condition).] Results from linear and nonlinear gyrokinetic simulations based on the Clebsch-type coordinate approach put forward in this paper will be presented in future publications. The same is true for applications to islands and ergodic regions, which require a detailed discussion with connection to the validity of the underlying physical model.

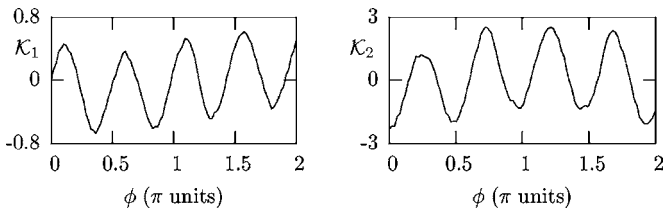

FIG. 7. Curvature terms $\mathcal{K}_1$ and $\mathcal{K}_2$ for W7-X, as computed numerically from a magnetohydrodynamic equilibrium via our coordinate approach.

ACKNOWLEDGMENTS

The authors would like to thank Dr. A. Mischenko and Dr. A. Mutzke for providing the equilibrium data for the tokamak configuration and W7-X stellarator, respectively, as well as Dr. A. Runov and Dr. R. Schneider for fruitful discussions.

APPENDIX: CLEBSCH-TYPE COORDINATES FOR A STRAIGHT CYLINDER

Here, we present an analytical realization of the Clebsch-type coordinates introduced in the main text for the case of magnetic surfaces with circular cross section, using standard results from the theory of differentiable curves. Particularly, we concentrate on the construction of two sets of Clebsch coordinates which provide exactly the same representation for the magnetic line. However, these sets differ in a quite important point; namely that the first one, (F^1_{fl},F^2_{fl}), is a flux coordinate system (i.e., the first coordinate is a flux-surface label), whereas the second one (F^1_{nf},F^2_{nf}) is not (i.e., none of the two coordinates is a flux-surface label).

Of course, the existence of two such systems is not a paradox, since the Clebsch representation is not unique. And as will be shown below, the two pairs of contravariant vectors are related merely through a plane rotation which preserves this representation. Now, in terms of the construction of (the gradients of) these coordinates, as discussed in Sec. II, the algorithm "selects" one particular coordinate system via the prescribed initial conditions. In the present case, it

turns out that for the standard initial conditions, Eq. (19), the resulting coordinate system is (F^1_{nf}, F^2_{nf}). The circular system is simple enough to be able to show that this flux coordinate system results if (and only if) the field-line tracing is started in the symmetry plane.

In the following, we consider a straight cylindrical system consisting of nested flux surfaces (e.g., a screw pinch) in order to prove the claims made above. We concentrate on a magnetic field line lying on a cylindrical flux surface of radius a and choose a Cartesian coordinate system such that its z axis coincides with the (straight) magnetic axis. Then the field line, seen as a circular helix, will have the representation

$$\mathbf{R}(\theta) = (a\cos\theta, a\sin\theta, s\theta), \tag{A1}$$

where θ is the poloidal angle and s is the pitch of the helix. (s is given in units of m, and the sign of s prescribes the orientation of the helix; for $s>0$, it is right-handed.) Now, we deduce the expressions for the (unit) vectors which constitute the Frenet moving trihedron. In particular, the tangent vector $\mathbf{t}=\mathbf{B}/B$, the normal $\mathbf{n}$ (radial direction), and the binormal $\mathbf{b}$ (diamagnetic direction) read

$$\mathbf{t} = \left(-\frac{a}{d}\sin\theta, \frac{a}{d}\cos\theta, \frac{s}{d}\right),$$

$$\mathbf{n} = (-\cos\theta, -\sin\theta, 0), \tag{A2}$$

$$\mathbf{b} = \left(\frac{s}{d}\sin\theta, -\frac{s}{d}\cos\theta, \frac{a}{d}\right),$$

where $d \equiv \sqrt{a^2+s^2}$.

Alternatively, it is possible to describe a field line through a set of equations

$$F^i(\mathbf{R}) = 0 \quad (i=1,2), \tag{A3}$$

where each equation represents a surface and, therefore, the curve results from the intersection of two surfaces. Then, the field line will have the representation

$$\mathbf{t} = K\nabla F^1 \times \nabla F^2, \tag{A4}$$

where K is a stream function, i.e., it has a constant value along the field line. As mentioned before, we intend to study two particular sets of coordinates in the following.

In the first case, we choose the first coordinate to be a flux-surface label,

$$F^1_{\mathrm{fl}} \equiv \sqrt{x^2+y^2} - a, \quad F^2_{\mathrm{fl}} \equiv \frac{a}{s}(s\arctan(y/x) - z). \tag{A5}$$

The scaling factor in the second coordinate will be justified below. Now, the relevant gradients (contravariant vectors) become

$$\nabla F^1_{\mathrm{fl}} = -\mathbf{n}, \quad \nabla F^2_{\mathrm{fl}} = -\frac{d}{s}\mathbf{b}, \tag{A6}$$

which confirms that F^1_{fl} is a flux-surface label. Therefore, the tangent vector can be written as

$$\mathbf{t} = \frac{s}{d}\nabla F^1_{\mathrm{fl}} \times \nabla F^2_{\mathrm{fl}}. \tag{A7}$$

Notice that the two representations (A7) and (A4) are equivalent, since the Jacobian is not zero,

$$J = \left|\frac{\partial(x,y)}{\partial(F^1_{\mathrm{fl}}, F^2_{\mathrm{fl}})}\right| = 1. \tag{A8}$$

In fact, $K=s/d=Jt_3$, which is the equivalent of JB^ϕ in the representation (4) for the magnetic field.

In the second case, we will obtain the same results, but this time for the surfaces

$$F^1_{\mathrm{nf}} \equiv x - a\cos(z/s), \quad F^2_{\mathrm{nf}} \equiv y - a\sin(z/s). \tag{A9}$$

The Jacobian of this transformation is again equal to unity. Now, the contravariant vectors read

$$\nabla F^1_{\mathrm{nf}} = 1, 0, \left(\frac{a}{s}\sin\theta\right) = \left(1, 0, -\frac{t_1}{t_3}\right),$$

$$\nabla F^2_{\mathrm{nf}} = 0, 1, \left(-\frac{a}{s}\cos\theta\right) = \left(0, 1, -\frac{t_2}{t_3}\right), \tag{A10}$$

and the representation for the field line becomes

$$\mathbf{t} = \frac{s}{d}\nabla F^1_{\mathrm{nf}} \times \nabla F^2_{\mathrm{nf}}, \tag{A11}$$

which is identical to Eq. (A7). (This result justifies the scaling factor we introduced in F^2_{fl} beforehand.) The pair of contravariant vectors $(\nabla F^1_{\mathrm{nf}}, \nabla^2_{\mathrm{nf}})$ is related to the pair $(\nabla F^1_{\mathrm{nf}}, \nabla^2_{\mathrm{nf}})$ through a plane rotation, since it holds

$$\nabla F^1_{\mathrm{nf}} = \cos\theta\nabla F^1_{\mathrm{fl}} - \sin\theta\nabla F^2_{\mathrm{fl}},$$

$$\nabla F^2_{\mathrm{nf}} = \sin\theta\nabla F^1_{\mathrm{fl}} - \cos\theta\nabla F^2_{\mathrm{fl}}. \tag{A12}$$

This implies that neither of the coordinates F^1_{nf} and F^2_{nf} is a flux-surface label, i.e., always directed along $\mathbf{n}$.

If Eq. (A10) is chosen as an initial condition for Eq. (16), the coordinate approach discussed in this paper will yield $(F^1_{\mathrm{nf}}, F^2_{\mathrm{nf}})$. If the initial conditions are chosen according to Eq. (A6), on the other hand, the flux coordinate system $(F^1_{\mathrm{fl}}, F^2_{\mathrm{fl}})$ will be retrieved. For complicated geometries, this practice becomes cumbersome, however, since the Frenet vectors have to be determined at the starting point of the tracing. A way of bypassing this inconvenience is to notice that in the symmetry plane, Eq. (A12) reduces to

$$\nabla F^1_{\mathrm{nf}}(\theta=0) = \nabla F^1_{\mathrm{fl}}(\theta=0) = (1,0,0),$$

$$\nabla F^2_{\mathrm{nf}}(\theta=0) = \nabla F^2_{\mathrm{fl}}(\theta=0) = \left(0, 1-\frac{t_2}{t_3}\right). \tag{A13}$$

In the context of the construction algorithm, this result states that, at least for the case of circular surfaces, if the tracing procedure starts in the midplane, where the condition $B^r=0$ holds (implying that ∇r is normal to the surface), then the modified initial conditions (20) provide as an exact solution the flux coordinate system $(F^1_{\mathrm{fl}}, F^2_{\mathrm{fl}})$.

As a final point, we would like to put Eq. (A13) in a more general context. Starting from the flux coordinate system $(F_{\mathrm{fl}}^1, F_{\mathrm{fl}}^2)$, one can set up an infinite family of systems which preserves the Clebsch representation, defined as

$$G^1 \equiv F_{\mathrm{fl}}^1 + g(F_{\mathrm{fl}}^2), \quad G^2 \equiv F_{\mathrm{fl}}^2, \tag{A14}$$

where g is an arbitrary function. The coordinate G^1 is no longer a flux-surface label since it contains a dependence on the poloidal angle θ. Considering the way these coordinates are constructed, the particular form of the function g is prescribed by the initial condition for the gradient ∇G^1. Therefore we end up with a unique set of coordinates. Since we aim at the generation of a flux coordinate system—given the existence of nested magnetic surfaces—these initial conditions should suppress the dependence of G^1 on the second coordinate, by reducing the function g to zero (or, more generally, to a constant). Therefore, at the starting point, the contravariant vector should satisfy $\nabla G^1 = \nabla F_{\mathrm{fl}}^1 = -\mathbf{n}$, i.e., it should be normal to the flux surface.

[1] E. A. Frieman and L. Chen, Phys. Fluids **25**, 502 (1982).
[2] R. G. Littlejohn, J. Plasma Phys. **29**, 111 (1983).
[3] T. S. Hahm, W. W. Lee, and A. Brizard, Phys. Fluids **31**, 1940 (1988).
[4] A. Brizard, J. Plasma Phys. **41**, 541 (1989).
[5] K. V. Roberts and J. B. Taylor, Phys. Fluids **8**, 315 (1965).
[6] S. C. Cowley, R. M. Kulsrud, and R. Sudan, Phys. Fluids B **3**, 2767 (1991).
[7] M. A. Beer, S. C. Cowley, and G. W. Hammett, Phys. Plasmas **2**, 2687 (1995).
[8] P. C. Liewer, Nucl. Fusion **25**, 543 (1985).
[9] F. Jenko, W. Dorland, M. Kotschenreuther, and B. N. Rogers, Phys. Plasmas **7**, 1904 (2000).
[10] T. Dannert and F. Jenko, Phys. Plasmas **12**, 072309 (2005).
[11] A. Runov, S. V. Kasilov, N. McTaggart, R. Schneider, X. Bonnin, R. Zagórski, and D. Reiter, Nucl. Fusion **44**, 74 (2004).
[12] P. Devynck, Nucl. Fusion **42**, 697 (2002).
[13] R. C. Wolf, W. Biel, M. F. M. de Bock *et al.*, Nucl. Fusion **45**, 1700 (2005).
[14] E. Strumberger, J. Nucl. Mater. **266-269**, 1207 (1999).
[15] W. D. D'Haeseleer, W. N. G. Hitchon, J. D. Callen, and J. L. Shohet, *Flux Coordinates and Magnetic Field Structure* (Springer, Berlin, 1991).
[16] V. V. Nemov, Nucl. Fusion **28**, 1727 (1988).
[17] F. Jenko and B. Scott, Phys. Plasmas **6**, 2418 (1999).
[18] F. Jenko and B. Scott, Phys. Plasmas **6**, 2705 (1999).
[19] J. W. Connor, R. J. Hastie, and J. B. Taylor, Phys. Rev. Lett. **40**, 396 (1978).